Original paper

Folia Neuropathologica

MiR-484 promotes the malignant progression of glioma by inhibiting CDKN2A expression

Yingrui Gu*, Hongbing Lei*, Peipei Ma, Yi Chen

Department of Neurosurgery, The First Affiliated Hospital of China Naval Medical University, Shanghai, China

*Yingrui Gu and Hongbing Lei contributed equally to this work.

Folia Neuropathol 2023; 61 (3): 249-265 *DOI: https://doi.org/10.5114/fn.2023.130002*

Abstract

Introduction: *Cyclin Dependent Kinase Inhibitor 2A (CDKN2A) is involved in glioma progression, but the specific molecular mechanism of CDKN2A in glioma cell migration and invasion needs to be further explored.*

Material and methods: *Data related to CDKN2A expression and glioma overall survival were obtained from The Cancer Genome Atlas (TCGA) database. Then, CDKN2A expression in glioma tissues/cells or paracancer tissues/astrocytes was measured by quantitative reverse transcription polymerase chain reaction (qRT-PCR) or Western blot. Afterwards, Wound healing, Transwell and tube formation assay were performed to identify the invasion, migration and angiogenesis of glioma cells, respectively. TargetScan database predicted the targeted binding between miR-484 and CDKN2A, which was verified by dual luciferase reporter gene assay. Western blot and qRT-PCR were performed to detect the expression of VEGF, E-cadherin, N-cadherin and Vimentin in glioma cells.*

Results: *CDKN2A was low-expressed in glioma tissue/cells as compared to paracancer tissue/astrocytes, and was strongly associated to the poor prognosis of glioma. Further studies found that down-regulation of CDKN2A could promote migration, invasion and angiogenesis of glioma cells. Besides, miR-484 was high-expressed in glioma cells compared to astrocytes. Up-regulation of miR-484 could enhance migration, invasion and angiogenesis of glioma cells. In addition, up-regulated miR-484 suppressed the expression of E-cadherin, and promoted the expression of N-cadherin, Vimentin and VEGF. However, there was negative regulation of miR-484 and CDKN2A, and CDKN2A could partially offset the effect of miR-484.*

Conclusions: *MiR-484 promoted cell migration, invasion and angiogenesis by inhibiting CDKN2A expression.*

Key words: *CDKN2A, miR-484, glioma, migration, invasion, angiogenesis.*

Introduction

Gliomas, which originate from glial cells in the brain, are the most common intracranial tumours (accounting for about 46% of intracranial tumours) [6,29,35]. Generally, the glioma often occurs at the age of 10-20 or 30-40. The symptoms of early glioma are not obvious, and the malignant degree of advanced glioma is very high [13,14]. Despite great progress in the treatment of glioma, the survival rate of glioma patients is still not very high, and the median survival time is only 15 months [1,8,12]. Therefore, new target therapeutic molecules and treatments have been promoted to be of vital importance.

Cyclin Dependent Kinase Inhibitor 2A (CDKN2A) is a protein-coding gene that is frequently deleted and mutated in a variety of tumours and is considered as an important tumour suppressor gene [25]. Studies have shown that CDKN2A is homozygous deficient in 50% of tumours, and low expression of CDKN2A is closely related to poor prognosis of the tumours [3]. Thus,

Communicating author:

Yi Chen, Department of Neurosurgery, The First Affiliated Hospital of China Naval Medical University, 168 Changhai Road, Yangpu District, Shanghai, 200433, China, phone: 86-021-31161795, e-mail: chyi_ych@163.com

CDKN2A has a definite role in glioma. A meta-analysis of 24,077 patients by Qi *et al.* showed that CDKN2A/B RS4977756 polymorphism could increase the risk of glioma [22]. Besides, CDKN2A has been shown to act as a negative regulator of cell proliferation through strong interactions with CDK4 and CDK6 [26]. However, the metastasis of glioma cells is an important factor in the poor prognosis of glioma [26]. Whether CDKN2A is involved in the migration and invasion of glioma cells needs further investigation.

MiR-484 is a non-coding short RNA (20-24 nt) that generally participates in the post-transcriptional regulation of gene expression in multicellular organisms by affecting the stability and translation of mRNA [7]. The study of Yi *et al.* suggested that miR-484 was negatively correlated with the overall survival of glioma patients [34]. Bioinformatics provides evidence that miR-484 could bind to CDKN2A. Perhaps miR-484 could negatively regulate CDKN2A involvement in glioma progression.

We hypothesized that miR-484 could target CDKN2A, thereby regulate the progression of glioma. This study aimed to explore the action mechanism of miR-484 and CDKN2A in the development of glioma, and to provide a theoretical basis for the diagnosis and precision treatment of glioma.

Material and methods

Ethics statement

The glioma tissues and its adjacent tissues were obtained from 65 glioma patients diagnosed in the First Affiliated Hospital of China Naval Medical University between March 2019 and March 2020. The study has been approved by the Ethics Committee of the First Affiliated Hospital of China Naval Medical University. Prior to tissue collection, all patients had signed informed consent.

Bioinformatics analysis

The CDKN2A expression profiles of glioma were analysed based on TCGA (The Cancer Genome Atlas) (http://cancergenome.nih.gov/) datasets [5]. The latest mRNASeq data for glioma were used for the survival analysis. miRanda (www.microrna.org) and TargetScan (http://www.targetscan.org/vert_72/) were performed to predict the relationship of CDKN2A and miR-484 [19].

Cell culture

The cell lines of HUVECs and human glioma cell lines (T98G, A172, LN-229 and U-87MG) were obtained from ATCC (Shanghai, China), while normal astrocytes (HEB and NHA) and human glioma cell line (U-251MG) were purchased from Shanghai Cell Bank (Shanghai, China). All cells were maintained in DMEM (12491-015, Gibco, USA) medium containing 10% foetal bovine serum (FBS, 10099-141, Gibco, USA) and 1% penicillin-streptomycin (15070063, Gibco, USA) in an incubator of 5% CO_2 at 37°C.

Cell transfection

MiR-484 inhibitor (miR20002174-1-5, RIBOBIO, China), inhibitor control (miR0190520020126, RIBOBIO, China), miR-484 mimics (miR10002174-1-5, RIBOBIO, China) and mimics control (miR1N0000001-1-5, RIBOBIO, China) were purchased from RIBOBIO (Guangdong, China), while si-NC (5'-UUCUCCGAACGUCACGU-3'), siCDKN2A (5'-GCGCUGCCCAACGCACCGAAU-3'), NC (C05001) and CDKN2A (NM_000077.5) were designed and constructed by GenePharma (Shanghai, China). The cells of LN-229 and U-251MG were cultured in low-FBS DMEM medium (without penicillin-streptomycin) in an incubator (5% CO_2, 37°C) for 24 h. The cells were planted on a 6-well plate with 3×10^5 cells/well. Cell transfection begins when the degree of cell fusion reaches 70-80%. Briefly, 10 µl of Lipofectamine 2000 (Lipo-2000; 11668-027, Invitrogen, USA), 4 µg of si-NC, siCDKN2A, NC, CDKN2A, scramble (mimics control/inhibitor control), miR-484 mimics and miR-484 inhibitor were diluted with 250 µl of Opti-MEM, respectively. After incubation for 5 min, si-NC, siCDKN2A, CDKN2A, NC, scramble (mimics control/inhibitor control), miR-484 mimics and miR-424-5p inhibitor and Lipo-2000 were mixed at room temperature for 20 min. Afterwards, the mixture was added to the medium for 6 h and then replaced.

Quantitative reverse transcription polymerase chain reaction (qRT-PCR)

Total RNA isolation was done using Trizol reagent (15596-018, Invitrogen, USA). However, the total miRNAs isolated by miRcute miRNA Isolation Kit (DP501, Tiangen, China) provided by Tiangen (Beijing, China). The purity of RNA was determined by a NanoDrop8000 spectrophotometer and the RNA samples used in this study reached 1.8-2.0 (A260/280). Then, the RNA reverse transcribed into cDNA using a Revert Aid First Strand cDNA synthesis kit (RR047AA, TaKaRa, Japan), and miRNA reverse transcribed into cDNA using the Bulge-Loop miRNA qRT-PCR Starter Kit. The sequences of CDKN2A and miR-484 was shown in Table I. GAPDH was the internal control of CDKN2A, VEGF, E-cadherin, N-cadherin and Vimentin, while U6 was the internal control of miR-484, miR-760, miR-155, miR-566. The progress of qPCR is as follows: the cDNA was diluted to double the volume, and 2 µl cDNA dilution solution was

Table I. Specific primer sequences for qRT-PCR

Gene	Primer sequence	Species
miR-484	5'-GTCGTATCCAGTGCGTGTCGTGGAGTCGGC AATTGCACTGGATACGACATCGGG-3' (RT) 5'-GCCGAGTCAGGCTCAGTCCCCT-3' 5'-CAGTGCGTGTCGTGGAGT-3'	Human
miR-760	5'-GTCGTATCCAGTGCGTGTCGTGGAGTCGGC AATTGCACTGGATACGACTCCCCA-3' (RT) 5'-TCGGCAGGCGGCTCTGGGTCT-3' 5'-CAGTGCGTGTCGTGGAGT-3'	Human
miR-155	5'-GTCGTATCCAGTGCGTGTCGTGGAGTCGGC AATTGCACTGGATACGACAACCCC-3' (RT) 5'-GCCGAGTTAATGCTAATCGTGA-3' 5'-GGCCAACCGCGAGAAGATGTTTTTTTT -3'	Human
miR-566	5'-GTCGTATCCAGTGCGTGTCGTGGAGTCGGC AATTGCACTGGATACGACGTTGGG-3' (RT) 5'-TCGGCAGGGCGCCTGTGATCCC-3' 5'-CTCAACTGGTGTCGTGGA-3'	Human
U6	5'-GTTGGCTCTGGTGCAGGGTCCGAGGTATTCG CACCAGAGCCAACAAAATATGG-3' (RT) 5'-ATTGGAACGATACAGAGAAGATT-3' 5'-GGAACGCTTCACGAATTTG-3'	Human
CDKN2A	5'-CAACGCACCGAATAGTTACGG-3' 5'-AACTTCGTCCTCCAGAGTCGC-3'	Human
VEGF	5'-AGGGCAGAATCATCACGAAGT-3' 5'-AGGGTCTCGATTGGATGGCA-3'	Human
E-cadherin	5'-CGAGAGCTACACGTTCACGG-3' 5'-GGGTGTCGAGGGAAAAATAGG-3'	Human
N-cadherin	5'-TCAGGCGTCTGTAGAGGCTT-3' 5'-ATGCACATCCTTCGATAAGACTG-3'	Human
Vimentin	5'-GACGCCAYCAACACCGAGTT-3' 5'-CTTTGTCGTTGGTTAGCTGGT-3'	Human
GAPDH	5'-CCACTCCTCCACCTTTGAC-3' 5'-ACCCTGTTGCTGTAGCCA-3'	Human

added to 10 µl SYBR Premix Ex TaqII™ (2×) (RR036A, TaKaRa, Japan). Afterwards, 0.2 mol/l primers were followed to add into the reaction system. Finally, the 20 µl reaction system is filled with double distilled water. The modified system was amplified in 7900 Real-Time PCR System (Biosystems, Foster City, USA) with the reaction conditions: 95°C for 30 s; 40 cycles include: 95°C for 5 s and 60°C for 30 s.

Western blot

The total protein was extracted from tissues and cells by RIPA reagent (P0013B, Beyotime Biotechnology, China) containing 1% protease inhibitor (P1030, Beyotime Biotechnology, China) and 2% phosphatase inhibitor (P1081, Beyotime Biotechnology, China). Then, BCA kit (P0012, Beyotime Biotechnology, Shanghai, China) was performed to measure the concentration of these samples. Afterwards, 30 µg of sample protein was resolved by 10% SDS-PAGE (sodium dodecyl sulfate-polyacrylamide gel electrophoresis) (P0690, Beyotime Biotechnology, China) and the marker (PR1910, Solarbio, China) was used to mark the molecular weight of the protein. The proteins were then transferred to polyvinylidene fluoride membrane (ISEQ00010/IPVH00010, MILLIPORE, USA). The membrane was blocked by 5% skimmed milk. After incubation for 1 h, the membrane was washed by TBST for 5 min and incubation by primary antibodies (CDKN2A: ab201980, 1 : 1000, Abcam; VEGF: ab46154, 1 : 5000, Abcam; E-cadherin: ab40772, 1 : 20,000, Abcam; N-cadherin: ab18203, 1 : 1000, Abcam; Vimentin: ab92547, 1 : 2000, Abcam; GAPDH: ab8245, 1 : 5000, Abcam) at 4°C overnight. The second day, primary antibody was recycled. Then, membrane was washed by TBST for 4 times (for 5 min each) and incubated with the secondary antibody (ab6721, 1 : 10000, Abcam) (incubated for 1 h at room temperature). Finally, the enhanced chemi-

luminescence solution (WBKLS0500, MILLIPORE, USA) was added to the band and the strip was visualized by the detection system. Image J (1.8.0, National Institutes of Health, Germany) is used to analyse the grey value of the strip.

Wound healing assay

The cells were seeded in a 6-well plate with 3×10^5 cells/well. When cells fusion reached 80-90%, the wounding healing assay was begun. A pipette tip (200 µl) was used to cause the wound, and the damage cells were washed out by PBS. Afterwards, the cells were continued to be cultured in an incubator (5% CO_2, 37°C) with FBS-free DMEM medium. The wound distance was recorded by invert microscope (100×) (NIB620, Boshida, China) at 0 h and 24 h. The scratch-healing areas were calculated using Image J and the following formula: Scratch-healing (%) = (initial scratch area – final scratch area)/initial scratch area × 100.

Transwell assay

The Bio-Coat Cell Migration Chamber (Corning, Corning, NY, USA) containing a 24-well plate containing an 8 µm-pore filter cell culture insert was performed in this assay. Firstly, 70 µl of matrix glue (diluted with DMEM: 1 : 4) was spread on the upper chamber and then incubated in the incubator for 3 h. Then, 3×10^5 cells were re-suspended with 500 µl FBS-free DMEM medium and transferred to the upper chamber. Meanwhile, 500 µl DMEM (including 20% FBS) was placed in the lower chamber. The chambers were continued incubation in the incubator (5% CO_2, 37°C) for 24 h. Afterwards, the non-invasive cells were rubbed by a cotton swab and the invasive cells were fixed with 4% paraformaldehyde (P0099-100 ml, Beyotime Biotechnology, China) for 20 min and stained with crystal violet (C0121, Beyotime Biotechnology, China) for 30 min. Cell counts were recorded for randomly selected cells from 5 microscope fields (100×) (NIB620, Boshida, China).

Tube formation assay

Firstly, Matrigel (BD Biosciences, MA, USA) was spread on 96-well plates and incubated for 1 h at 37°C. Then, the medium of culture transfected cells for 24 h were re-suspended HUVECs cells. Afterwards, 100 µl of HUVECs (1.5×10^5 cells/ml) were implanted in the 96-well plates (coated with matrix glue). The plates continued incubation at 37°C for 4 h, the presence of tubular structures was observed by an inverted microscope (NIB620, Boshida, China). The length of the tube was calculated using image J software (1.8.0, National Institutes of Health, Germany).

Dual-luciferase reporter gene assay

NCBI (https://www.ncbi.nlm.nih.gov/) provided the 3'-UTR sequence of CDKN2A, and then the 3'-UTR sequence was connected with the pmirGLO luciferase vector (E1751, Promega, USA) to conduct the pmirGLO-CDKN2A-3'-UTR recombinant. Point mutations were generated in the miR-484 binding site of the CDKN2A and produced pmirGLO-CDKN2A-3'-UTR-MUT.

LN-229 and U-251MG cells were cultured in a 96-well plate. When the degree of cell fusion reaches 60-80%, the reporter gene constructs (pmirGLO-CDKN2A-3'-UTR and pmirGLO-CDKN2A-3'-UTR-MUT) and miR-484 mimics could be co-transfected into the cells. The cells were collected and the luciferase activity was determined according to the manufacturer's recommendations using the dual luciferase reporter gene detection system (E2940, Promega, USA) after being transfected for 24 h.

Immunohistochemistry

The brain tissue was fixed in 4% paraformaldehyde, embedded in paraffin, and five-micron-thick sections were prepared. Sections were stained with an antibody against CDKN2A. Brown staining in cells was considered as positive signal.

Statistical analysis

The data of this study were analysed by SPSS19.0. All data were expressed as mean ±SD. One-way ANOVA was performed for multi-group comparison and then performed by Dunnett or Tukey test. The paired *t*-test was used for paired samples. $P < 0.05$ was considered to indicate statistically significant differences.

Results

CDKN2A is low-expressed in glioma tissues/cells, which is closely related to the good prognosis of glioma

The mRNA expression of CDKN2A and survival information of patients with glioma patients was download from the TCGA database. Overall survival curve revealed that glioma patients with low CDKN2A expression had a shorter overall survival than those with high CDKN2A expression (Fig. 1A, $p < 0.001$). Then, the mRNA expression of CDKN2A in 65 pairs of glioma tissues/cells and normal paracancer tissues/normal astrocytes were measured by qRT-PCR. As can be seen in Figure 1B and 1C, CDKN2A had low expression in glioma tissues as compared to adjacent tissue ($p < 0.01$). Besides, CDKN2A expression was lower in glioma cells, including T98G, A172, LN229, U-87MG and U-251MG cells, than that in normal astrocytes

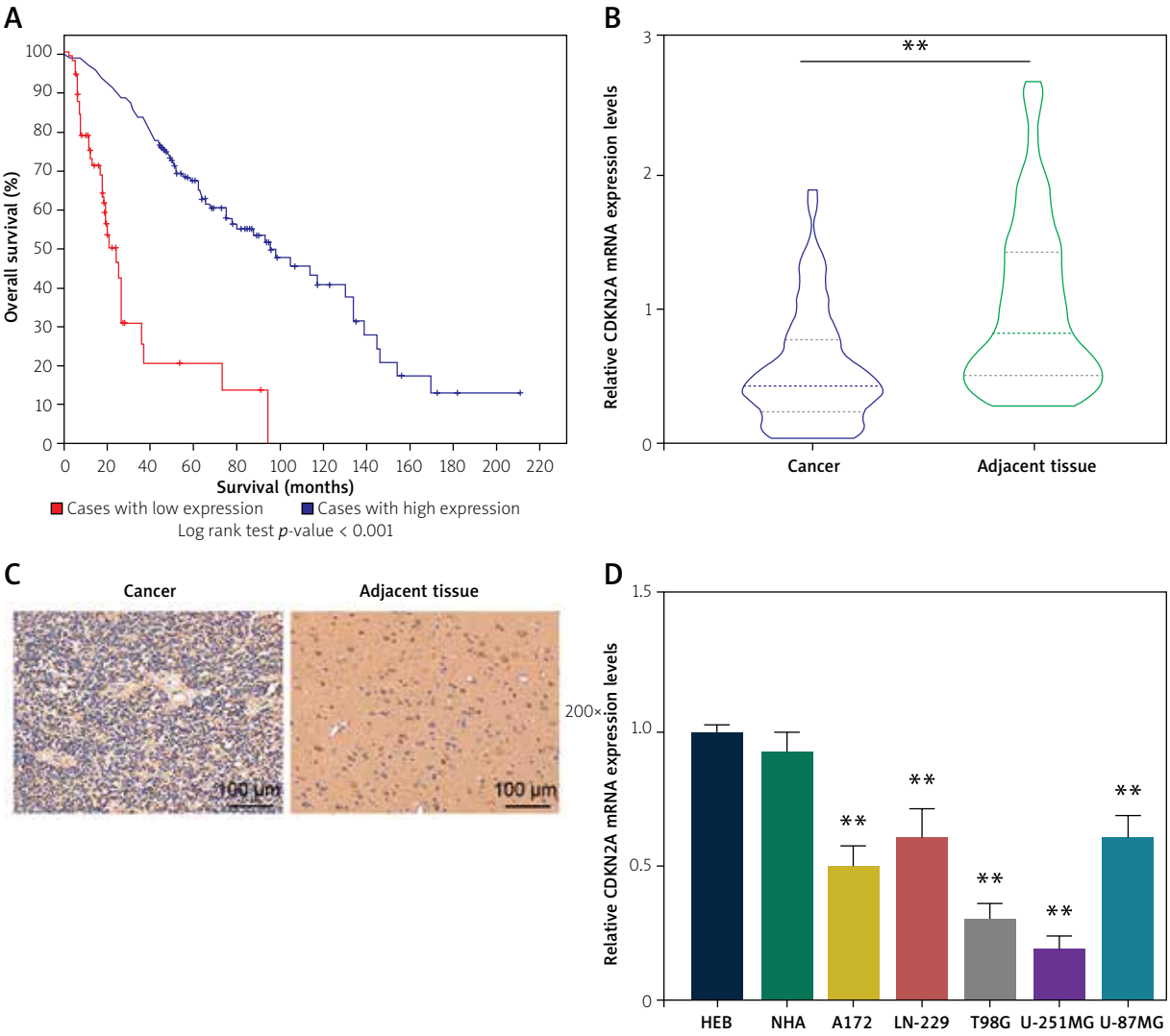

Fig. 1. Low expression CDKN2A in glioma is closely related to the poor prognosis of glioma. **A**) TCGA database was used to analyse the relationship between CDKN2A and the overall survival of glioma patients. **B**) The expression of CDKN2A in glioma tissues and adjacent tissues was detected by qRT-PCR; $n = 65$. * vs. Cancer, $^{**}p < 0.001$. **C**) Immunohistochemical staining of CDKN2A in glioma and adjacent tissues using anti-CDKN2A antibody. Images were captured at 200×, scale bar: 100 μm. **D**) The expression of CDKN2A in glioma cells (A172, LN-229, T98G, U-251MG and U-87MG) and normal astrocytes (HEB and NHA) was detected by qRT-PCR; $n = 3$. ** vs. HEB, $^{**}p < 0.001$.

(Fig. 1D, $p < 0.01$). Notably, among these five cell lines, the expression of CDKN2A was the highest in LN-229 and was the lowest in U-251MG. Thus, the two cell lines were performed as the subjects for later experiments.

Down-regulation of CDKN2A enhanced the migration, invasion and angiogenesis of LN-229 cells

The expression of CDKN2A in LN-229 was the highest among the 5 glioma cells, so we down-regulated the CDKN2A expression to verify the effect of CDKN2A in LN-229 cells. Both Western blot and qRT-PCR results showed that siCDKN2A reduced the expression of CDKN2A (Fig. 2A-C, $p < 0.001$). Then, we found that down-regulated CDKN2A could promote LN-299 cells migration and invasion by the Wound healing assay and Transwell assay (Fig. 2D, E, $p < 0.001$). Besides, we were surprised to find that siCDKN2A facilitated LN-299 cell angiogenesis (Fig. 2F, $p < 0.001$).

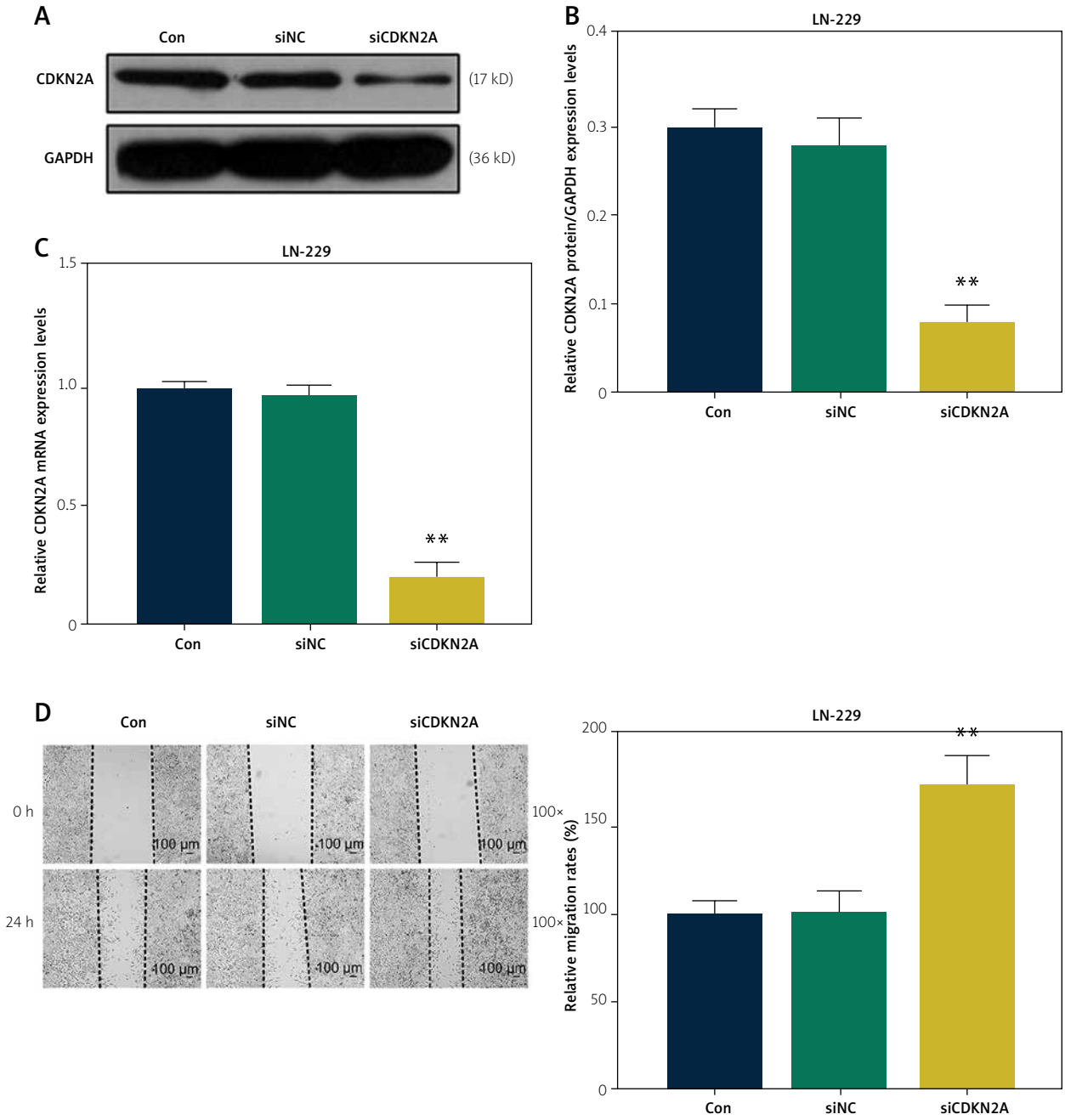

Fig. 2. Down-regulated CDKN2A expression enhanced LN-229 cell migration, invasion, and angiogenesis. **A**) Transfection efficiency of CDKN2A in LN-229 cells were detected by Western blot; $n = 3$. **B**) The signal intensities of CDKN2A were quantified; $n = 3$. **C**) Transfection efficiency of CDKN2A in LN-229 cells was detected by qRT-PCR; $n = 3$. **D**) Wound healing assay was used to detect the effect of CDKN2A on the migration of LN-229 cells. Scale: 100 µm, magnification: 100×; $n = 3$. ** vs. siNC, $^{**}p < 0.001$.

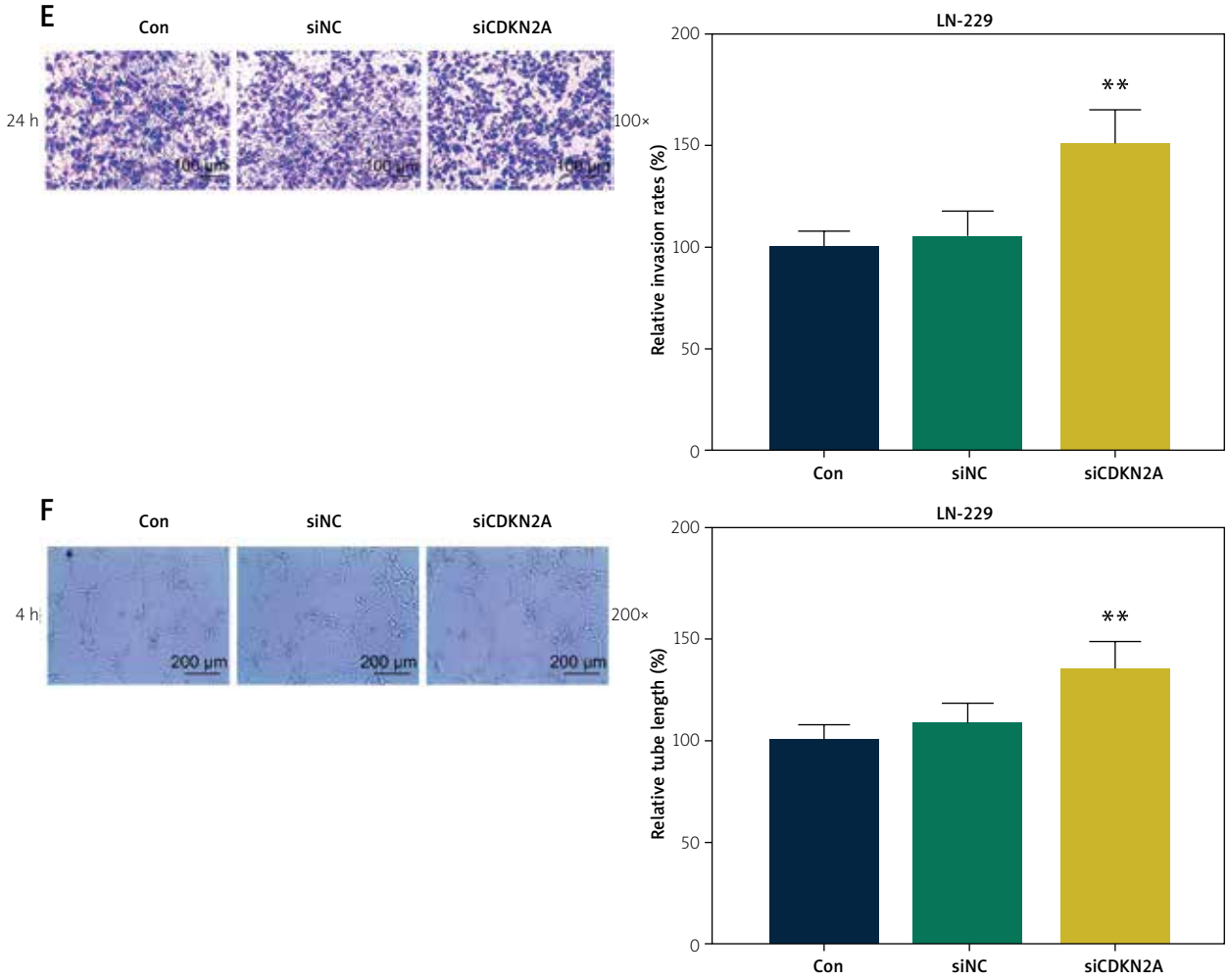

Fig. 2. Cont. **E**) Transwell assay was used to detect the effect of CDKN2A on the invasion of LN-229 cells. Scale: 100 µm, magnification: 100×; $n = 3$. **F**) Tube formation assay was used to detect the effect of CDKN2A on the angiogenesis of LC-229 cells. Scale: 200 µm, magnification: 200×; $n = 3$. ** vs. siNC, **$p < 0.001$.

Up-regulation of CDKN2A decreased the migration, invasion and angiogenesis of U-251MG cells

It is no surprise that we chose up-regulation of CDKN2A to detect its role in U-251MG cells, because CDKN2A was the least expressed in U-251MG cells among the 5 glioma cells. We also performed Western blot and qRT-PCR to measure the transfection efficiency of CDKN2A over-expression plasmids. As listed in Figure 3A-C, the expression of CDKN2A was enhanced as compared to the control group ($p < 0.001$). Afterwards, we demonstrated that up-regulated CDKN2A would decrease the migration and invasion of U-251MG cells by the Wound healing and Transwell assay (Fig. 3D, E, $p < 0.001$). In addition, the angiogenesis of U-251MG cells was suppressed after CDKN2A over-expression (Fig. 3F, $p < 0.001$).

miR-484 targeted CDKN2A *via* direct binding

Four candidate miRNAs bound to CDKN2A were finally determined by miRDB and TargetScan database. As shown in Figure 4A-D, miR-760, miR-155 and miR-566 were higher or lower expressed in human glioma cell line than normal astrocytes, while miR-484 was higher expressed in human glioma cell line than normal astrocytes ($p < 0.01$). Thus, among 4 miRNAs, only the expression of miR-484 was negatively correlated with CDKN2A, so we believe that miR-484 has a very important potential value in regulating CDKN2A (Fig. 4A-E, $p < 0.001$). Then, we verified the relationship of miR-484 and CDKN2A. As evident in Figure 4F and G, the luciferase activity of CDKN2A wild-type was lower than that of the CDKN2A and miR-484 binding site mutation group in both LN-229 and U-251MG cells

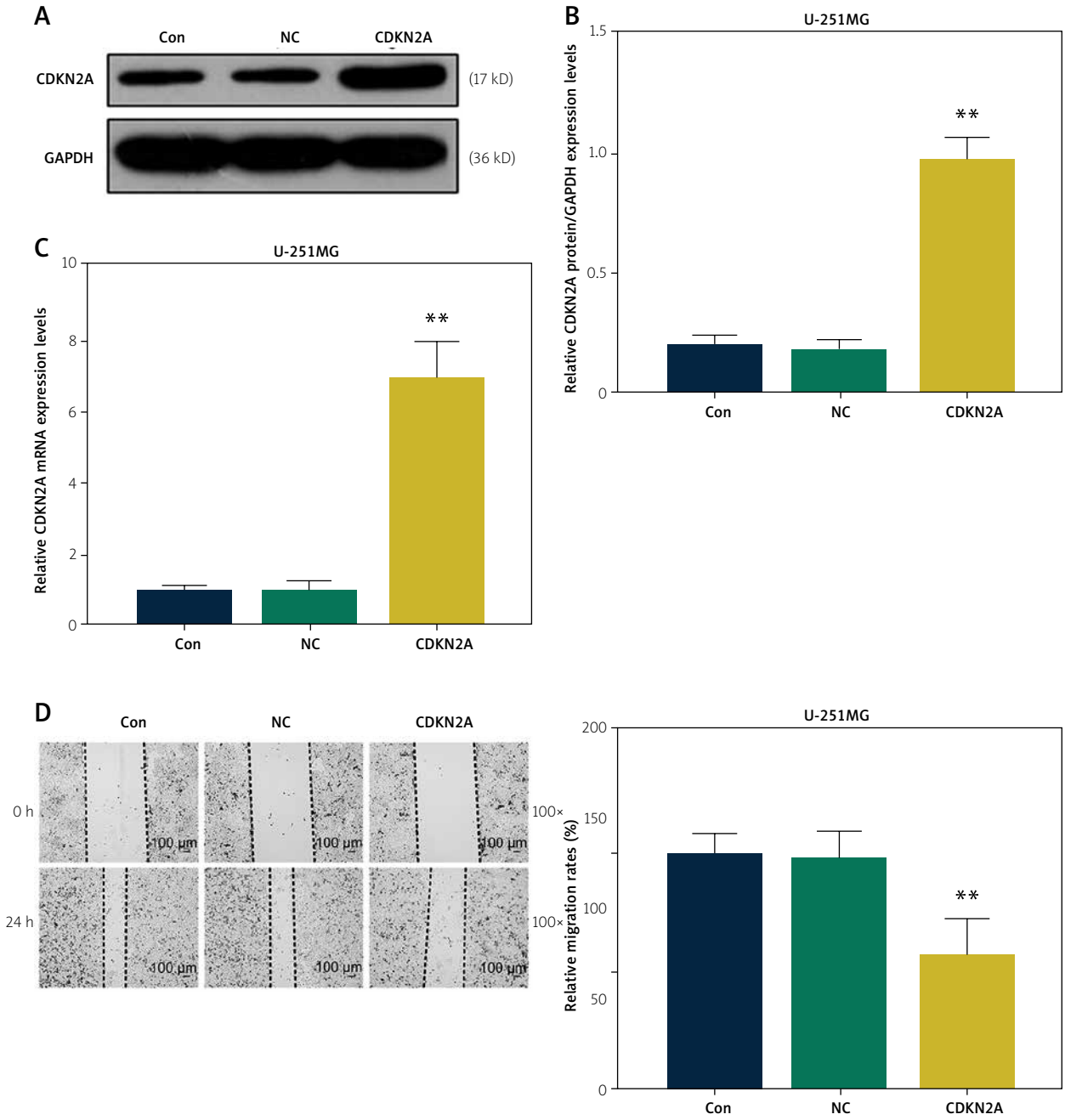

Fig. 3. Up-regulated CDKN2A expression decreased U-251MG cells migration, invasion, and angiogenesis. **A**) Transfection efficiency of CDKN2A in U-251MG cells were detected by Western blot; $n = 3$. **B**) The signal intensities of CDKN2A were quantified; $n = 3$. **C**) Transfection efficiency of CDKN2A in U-251MG cells was detected by qRT-PCR; $n = 3$. **D**) Wound healing assay was used to detect the effect of CDKN2A on the migration of U-251MG cells. Scale: 100 μm, magnification: 100×; $n = 3$. ** vs. NC, $^{**}p < 0.001$.

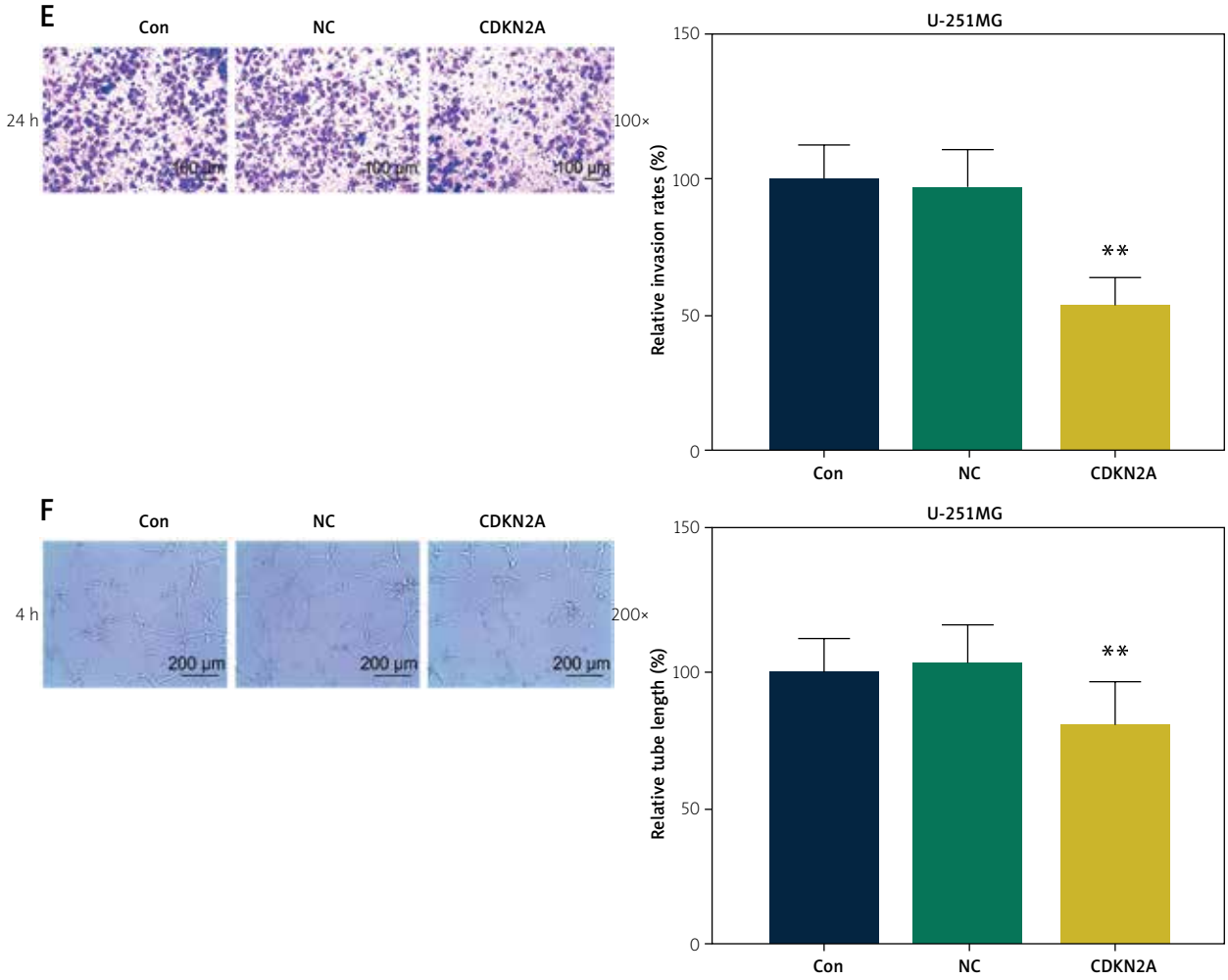

Fig. 3. Cont. **E**) Transwell assay was used to detect the effect of CDKN2A on the invasion of U-251MG cells. Scale: 100 μm, magnification: 100×; $n = 3$. **F**) Tube formation assay was used to detect the effect of CDKN2A on the angiogenesis of U-251MG cells. Scale: 200 μm, magnification: 200×; $n = 3$. ** vs. NC, **$p < 0.001$.

($p < 0.001$). The results indicated that miR-484 could target CDKN2A.

MiR-484 enhanced migration, invasion and angiogenesis of LN-229 cells by inhibiting the expression of CDKN2A

MiR-484 mimics promoted the expression of miR-484 (Fig. 5A, $p < 0.001$). CDKN2A overexpression had no effect on the expression of miR-484 (Fig. 5B, $p < 0.001$). Then, we found that miR-484 mimics could enhance the migration and invasion of LN-299 cells as compared to the control group. However, up-regulation of CDKN2A could partially counteract the effect of miR-484 mimics (Fig. 5C, D, $p < 0.001$). Meanwhile, miR-484 mimics could enhance the angiogenesis of LN-229 cells as compared to the control group, and CDKN2A over-expression could partially offset the effect (Fig. 5E, $p < 0.001$, $p < 0.05$). Besides, the expression of E-cadherin was inhibited, while VEGF, N-cadherin and Vimentin expressions were enhanced after LN-229 cells transfected with miR-484 mimics. Up-regulation of CDKN2A would partially offset the changes of E-cadherin, VEGF, N-cadherin and Vimentin expression caused by miR-484 mimics (Fig. 5F-H, $p < 0.001$). In summary, miR-484 enhanced LN-229 cells migration, invasion and angiogenesis by inhibiting the expression of CDKN2A.

Down-regulation of miR-484 decreased U-251MG cells migration, invasion and angiogenesis by promoting the expression of CDKN2A

The effect of miR-484 inhibitor was identified by qRT-PCR, and the results showed that miR-484 inhib-

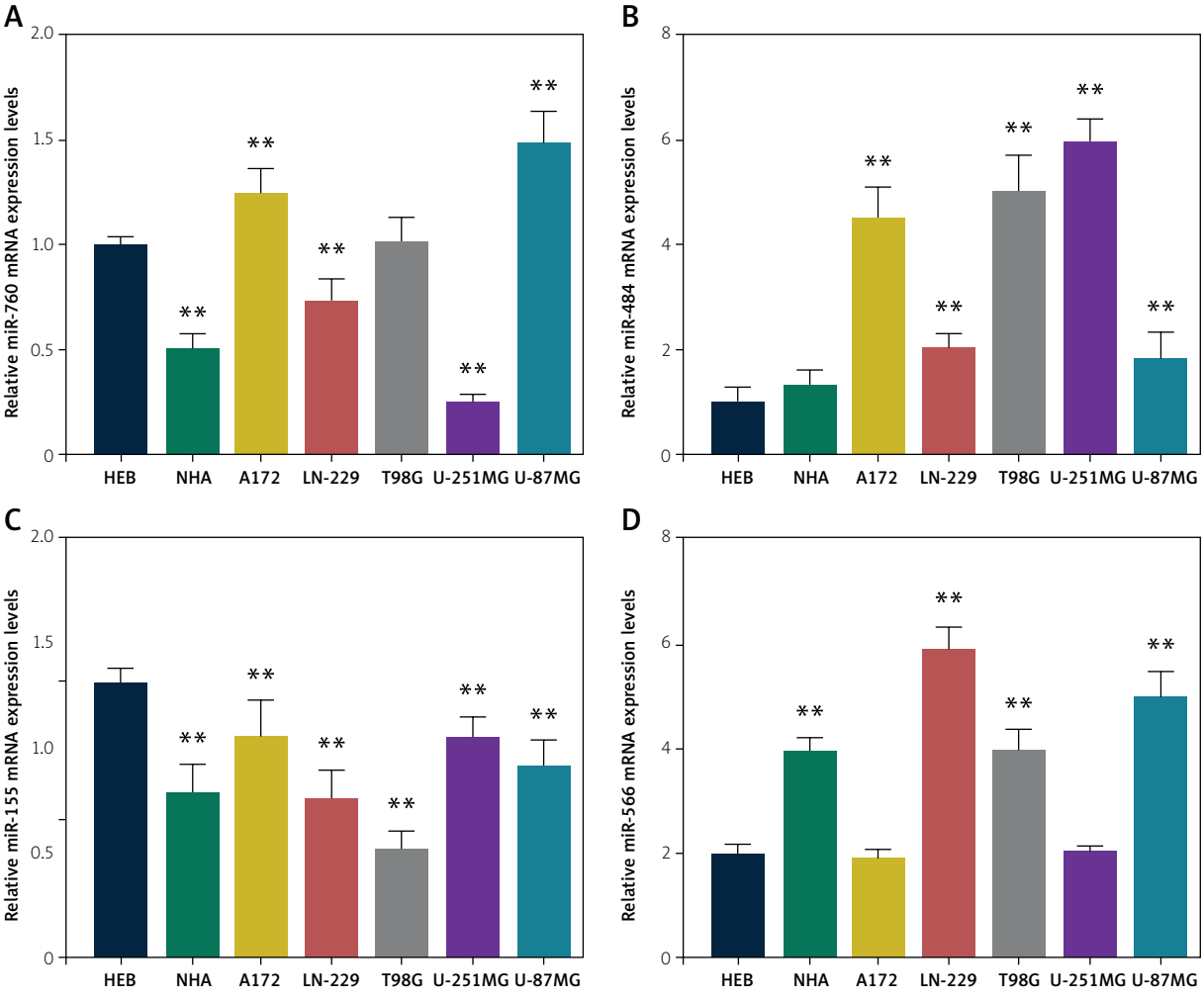

E

Position 32-39 of CDKN2A 3'UTR	5′	...CGCCGAGGAGCGCCAGAGCCUGA...
		|||| |||||||
hsa-miR-484	3′	UAGCCCUCCCCUGA--CUCGGACU

Fig. 4. miR-484 targeted CDKN2A *via* direct binding. **A**) The expression of miR-760 in glioma cells (A172, LN-229, T98G, U-251MG and U-87MG) and normal astrocytes (HEB and NHA) was detected by qRT-PCR; $n = 3$. ** vs. HEB, $^{**}p < 0.001$. **B**) The expression of miR-484 in glioma cells (A172, LN-229, T98G, U-251MG and U-87MG) and normal astrocytes (HEB and NHA) was detected by qRT-PCR; $n = 3$. ** vs. HEB, $^{**}p < 0.001$. **C**) The expression of miR-155 in glioma cells (A172, LN-229, T98G, U-251MG and U-87MG) and normal astrocytes (HEB and NHA) was detected by qRT-PCR; $n = 3$. ** vs. HEB, $^{**}p < 0.001$. **D**) The expression of miR-566 in glioma cells (A172, LN-229, T98G, U-251MG and U-87MG) and normal astrocytes (HEB and NHA) was detected by qRT-PCR; $n = 3$. ** vs. HEB, $^{**}p < 0.001$. **E**) TargetScan predicts the binding sites of miR-484 and CDKN2A.

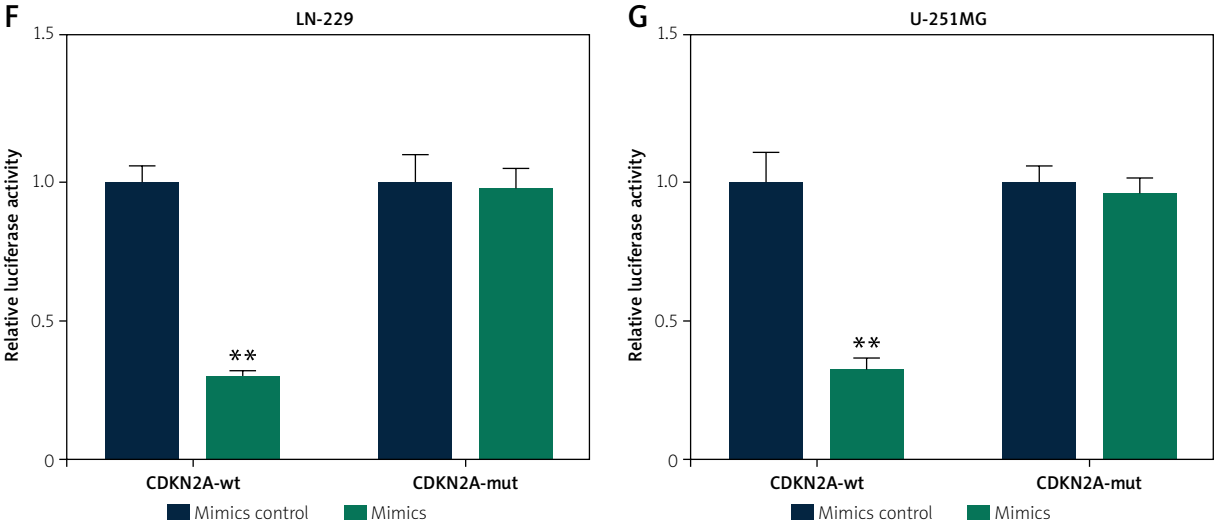

Fig. 4. Cont. **F**) Dual-luciferase reporter assay verified the targeted binding of miR-484 and CDKN2A in LN-229 cells; $n = 3$. ** vs. Mimics control, **$p < 0.001$. **G**) Dual-luciferase reporter assay verified the targeted binding of miR-484 and CDKN2A in U-251MG cells; $n = 3$. ** vs. Mimics control, **$p < 0.001$.

itor could decrease the expression of miR-484 (Fig. 6A, $p < 0.001$). Similarly, siCDKN2A had no effect on the expression of miR-484 (Fig. 6B, $p < 0.001$). Afterwards, we found that miR-484 inhibitor could decrease U-251MG cells migration, invasion and angiogenesis as compared to the control group. However, siCDKN2A attenuated the effect of miR-484 inhibitor on U-251MG cells migration, invasion and angiogenesis (Fig. 6C-E, $p < 0.001$). Besides, the expression of E-cadherin, VEGF, N-cadherin and Vimentin was also measured by Western blot and qRT-PCR. As shown in Figure 6F-H, compared to the control group, miR-484 inhibitor decreased the expression of VEGF, N-cadherin and Vimentin, while increased the expression of E-cadherin. Nonetheless, siCDKN2A partially counteract the changes of E-cadherin, VEGF, N-cadherin and Vimentin expression caused by miR-484 inhibitor (Fig. 6F-H, $p < 0.001$, $p < 0.05$).

Discussion

As a serious glioma, brain glioma has been a serious threat to people's life and health. Current treatments for gliomas include radiation, chemotherapy (temozolomide and PCV) or surgical resection, all of these methods are based on nonspecific targeting of proliferating cells [9]. However, gliomas are indistinguishable from normal tissue and are difficult to remove completely [30]. In addition, since glioma is not particularly sensitive to chemotherapy or radiation, it is very easy to relapse [17,37]. Therefore, glioma becomes one of the tumours with the worst prognosis, how to improve the therapeutic effect and prognosis of glioma has become a focus of clinical attention [15]. Fortunately, specific molecular targeted therapy for abnormal cell proliferation brings hope for the treatment of glioma, and finding new molecular targets becomes an urgent problem to solve.

The cell cycle is the basic process of cell life activity. Current studies have shown that there are key regulatory points between different phases of the cell cycle, including the regulatory point for entering S phase (G1 check point) and the regulatory point for entering M phase (G2 check point). Obviously, the G1 check point plays the vital role in the cell process. The network regulation of this check point is carried out by the interaction of cyclins, cyclin dependent kinases (CDKs) and cyclin dependent kinase inhibitors (CKIs) [23]. The core mechanism of the cell cycle is the expression of CDKs [16]. CDKN2A is an important CDK in the G1 phase, which can play a pivotal role in G1 control through the regulation of CDK4 and p53 in the G1 process of the cell cycle [24]. CDKN2A was found to be down-expressed in a variety of tumours, including gliomas, and its abnormal expression caught researchers' attention [18,21,33]. According to Appay *et al.* study, CDKN2A homozygous deletion is an important factor in the poor prognosis of gliomas [2]. Similarly, Sibin *et al.* also demonstrated that reduced CDKN2A expression is a marker of poor prognosis in malignant high-grade gliomas [26]. In our study, we found that low CDKN2A expression was closely associated with poor prognosis of glioma. In addition, CDKN2A was low expressed in both glioma tissues and glioma cells. These results are consistent with previous studies. Besides, we also found that CDKN2A silencing promoted migration, invasion and angiogenesis of gli-

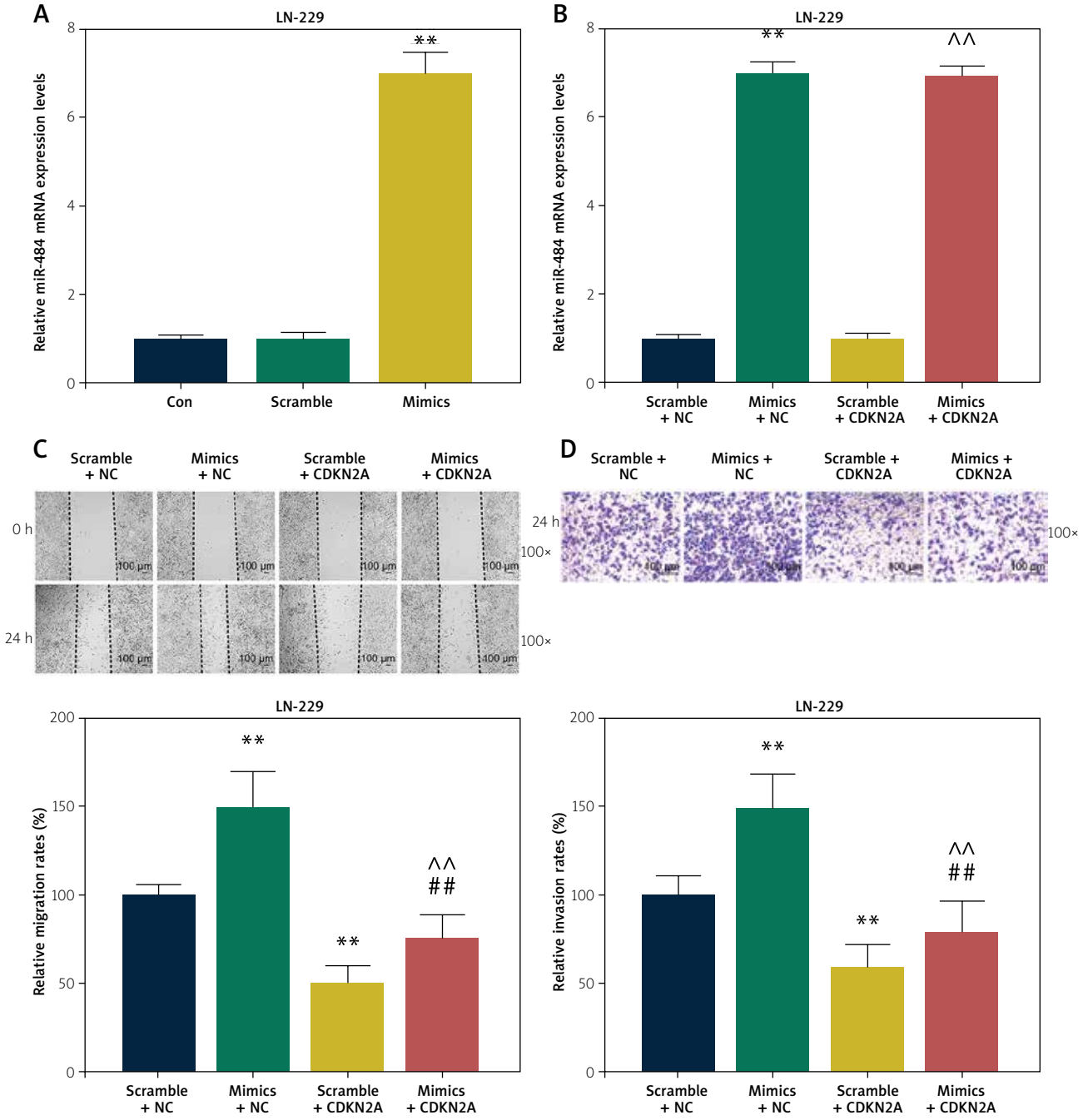

Fig. 5. MiR-484 enhanced LN-229 cells migration, invasion and angiogenesis by inhibiting the expression of CDKN2A. **A**) Transfection efficiency of miR-484 mimics in LN-229 cells was detected by qRT-PCR; $n = 3$. ** vs. Scramble, $^{**}p < 0.001$. **B**) The expression of miR-484 in LN-229 cells was detected by qRT-PCR; $n = 3$. ** vs. Scramble + NC, ^^ vs. Scramble + CDKN2A, $^{**}p < 0.001$, $^{\wedge\wedge}p < 0.001$. **C**) Wound healing assay was used to detect the effect of CDKN2A and miR-484 on the migration of LN-229 cells. Scale: 100 µm, magnification: 100×; $n = 3$. ** vs. Scramble + NC, ## vs. Mimics + NC, ^^ vs. Scramble + CDKN2A, $^{**}p < 0.001$, $^{\#\#}p < 0.001$, $^{\wedge\wedge}p < 0.001$. **D**) Transwell assay was used to detect the effect of CDKN2A and miR-484 on the invasion of LN-229 cells. Scale: 100 µm, magnification: 100×; $n = 3$. ** vs. Scramble + NC, ## vs. Mimics + NC, ^^ vs. Scramble + CDKN2A, $^{**}p < 0.001$, $^{\#\#}p < 0.001$, $^{\wedge\wedge}p < 0.001$

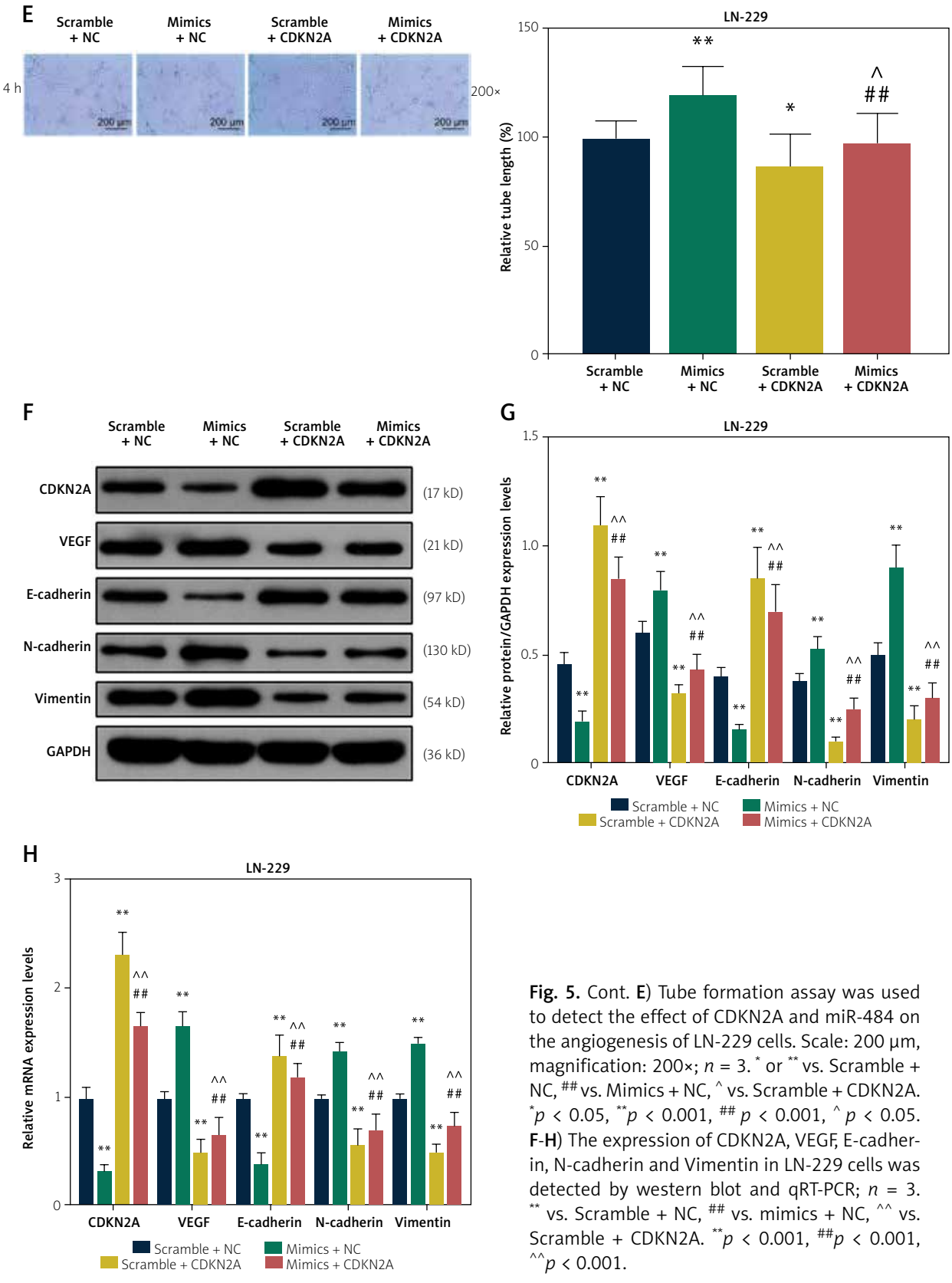

Fig. 5. Cont. **E**) Tube formation assay was used to detect the effect of CDKN2A and miR-484 on the angiogenesis of LN-229 cells. Scale: 200 μm, magnification: 200×; $n = 3$. * or ** vs. Scramble + NC, $^{\#\#}$ vs. Mimics + NC, $^{\wedge}$ vs. Scramble + CDKN2A. $^{*}p < 0.05$, $^{**}p < 0.001$, $^{\#\#}p < 0.001$, $^{\wedge}p < 0.05$. **F-H**) The expression of CDKN2A, VEGF, E-cadherin, N-cadherin and Vimentin in LN-229 cells was detected by western blot and qRT-PCR; $n = 3$. ** vs. Scramble + NC, $^{\#\#}$ vs. mimics + NC, $^{\wedge\wedge}$ vs. Scramble + CDKN2A. $^{**}p < 0.001$, $^{\#\#}p < 0.001$, $^{\wedge\wedge}p < 0.001$.

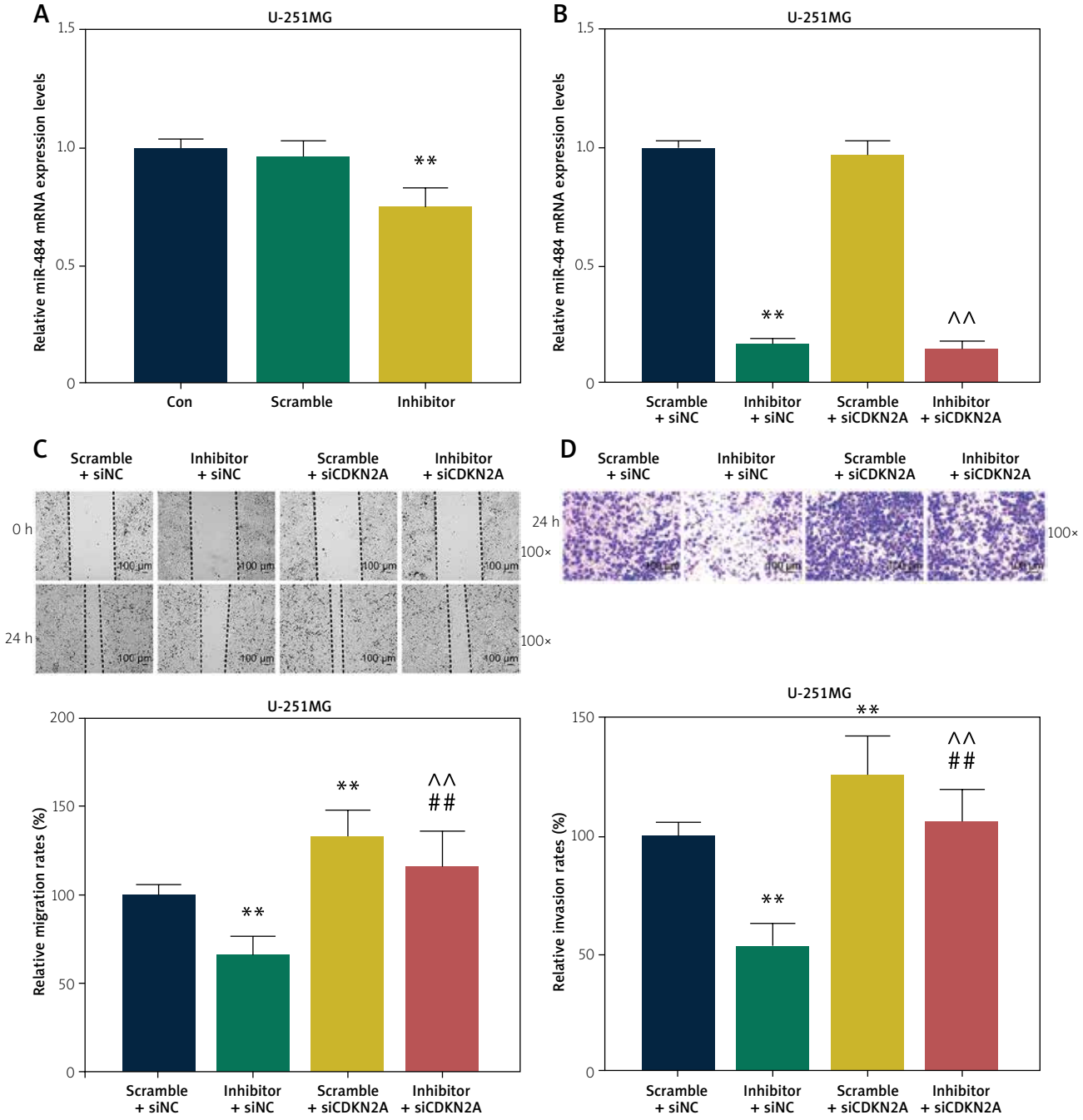

Fig. 6. Down-regulation of miR-484 decreased U-251MG cells migration, invasion and angiogenesis by promoting the expression of CDKN2A. **A**) Transfection efficiency of miR-484 inhibitor in U-251MG cells was detected by qRT-PCR; $n = 3$. ** vs. Scramble, $^{**}p < 0.001$. **B**) The expression of miR-484 in U-251MG cells was detected by qRT-PCR; $n = 3$. ** vs. Scramble + siNC, ^^ vs. Scramble + siCDKN2A, $^{**}p < 0.001$, $^{\wedge\wedge}p < 0.001$. **C**) Wound healing assay was used to detect the effect of CDKN2A and miR-484 on the migration of U-251MG cells. Scale: 100 µm, magnification: 100×; $n = 3$. ** vs. Scramble + siNC, ## vs. inhibitor + siNC, ^^ vs. Scramble + siCDKN2A, $^{**}p < 0.001$, $^{\#\#}p < 0.001$, $^{\wedge\wedge}p < 0.001$. **D**) Transwell assay was used to detect the effect of CDKN2A and miR-484 on the invasion of U-251MG cells. Scale: 100 µm, magnification: 100×; $n = 3$. ** vs. Scramble + siNC, ## vs. inhibitor + siNC, ^ vs. Scramble + siCDKN2A, $^{**}p < 0.001$, $^{\#\#}p < 0.001$, $^{\wedge\wedge}p < 0.001$.

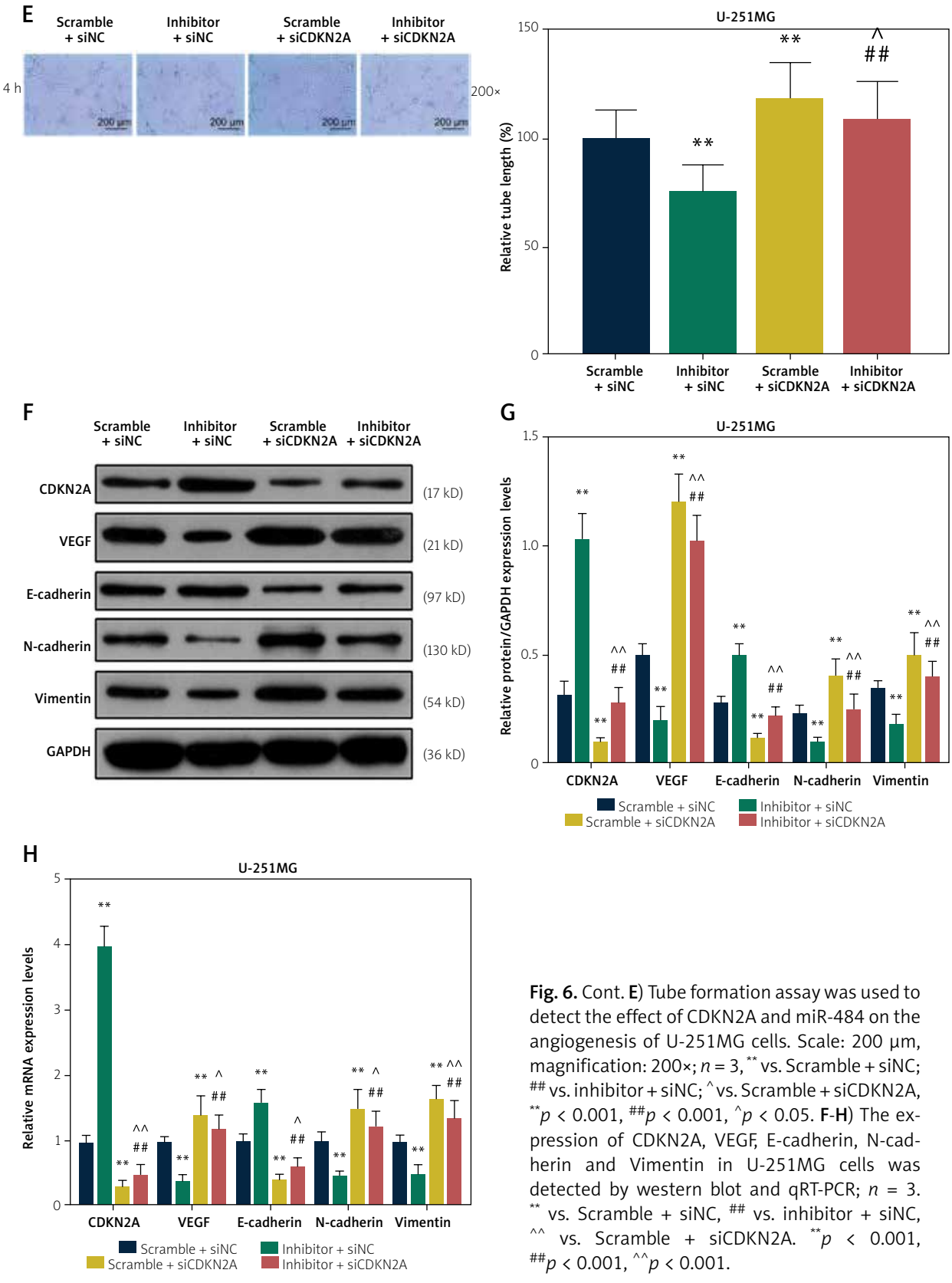

Fig. 6. Cont. **E**) Tube formation assay was used to detect the effect of CDKN2A and miR-484 on the angiogenesis of U-251MG cells. Scale: 200 μm, magnification: 200×; $n = 3$, ** vs. Scramble + siNC; ## vs. inhibitor + siNC; ^ vs. Scramble + siCDKN2A, $^{**}p < 0.001$, $^{\#\#}p < 0.001$, $^{\wedge}p < 0.05$. **F-H**) The expression of CDKN2A, VEGF, E-cadherin, N-cadherin and Vimentin in U-251MG cells was detected by western blot and qRT-PCR; $n = 3$. ** vs. Scramble + siNC, ## vs. inhibitor + siNC, ^^ vs. Scramble + siCDKN2A. $^{**}p < 0.001$, $^{\#\#}p < 0.001$, $^{\wedge\wedge}p < 0.001$.

oma cells. The above results suggested that CDKN2A plays a very vital role in the metastasis of glioma.

The development of bio-information has brought great help to the study of the molecular mechanism of glioma [10]. We selected four miRNAs with binding relationship to CDKN2A screened by TargetScan databases. TargetScan is a very valuable website that predicts gene targets regulated by miRNAs [19]. Further verification of normal human astrocytes and human glioma cells revealed that only miR-484 expression was negatively correlated with CDKN2A, so we speculated that miR-484 played a crucial role in the progression of glioma. Strikingly, Yi *et al.* found that the high expression of miR-484 could promote the initiation of glioma [34]. However, we also found that miR-484 promoted glioma cells migration, invasion and angiogenesis by inhibiting CDKN2A expression. To verify this result, the expressions of VEGF, E-cadherin, N-cadherin, and Vimentin were also detected. Some studies have pointed that E-cadherin, N-cadherin and Vimentin are markers of epithelial-mesenchymal transition (EMT), and which is an important mechanism of glioma invasion and metastasis [11,20,27,32,36]. Yang *et al.* found that down-regulation of PSMB8 would decrease the migration and proliferation of glioma cells by reducing the expression of Vimentin and N-cadherin and increasing the expression of E-cadherin [31]. Besides, VEGF is a key regulator of angiogenesis, affecting endothelial cell survival and function [36]. Sun *et al.* proved that miR-21 promotes the angiogenic ability of endothelial cells by promoting the expression of VEGF [28]. Therefore, the results of the changes of VEGF, E-cadherin, N-cadherin and Vimentin expression verified the conclusion that low CDKN2A expression promoted the angiogenesis, migration and invasion of glioma.

Our study demonstrated that miR-484 promotes glioma cells migration, invasion and angiogenesis by regulating CDKN2A, which demonstrated the molecular mechanism of glioma progression and provided a very valuable theoretical basis for the targeted therapy of glioma.

Disclosure

The authors report no conflict of interest.

References

1. Ahmed R, Oborski MJ, Hwang M, Lieberman FS, Mountz JM. Malignant gliomas: current perspectives in diagnosis, treatment, and early response assessment using advanced quantitative imaging methods. Cancer Manag Res 2014; 6: 149-170.
2. Appay R, Dehais C, Maurage CA, Alentorn A, Carpentier C, Colin C, Ducray F, Escande F, Idbaih A, Kamoun A, Marie Y, Mokhtari K, Tabouret E, Trabelsi N, Uro-Coste E, Delattre JY, Figarella-Branger D, POLA Network. CDKN2A homozygous deletion is a strong adverse prognosis factor in diffuse malignant IDH-mutant gliomas. Neuro Oncol 2019; 21: 1519-1528.
3. Bartels S, van Luttikhuizen JL, Christgen M, Mägel L, Luft A, Hänzelmann S, Lehmann U, Schlegelberger B, Leo F, Steinemann D, Kreipe H. CDKN2A loss and PIK3CA mutation in myoepithelial-like metaplastic breast cancer. J Pathol 2018; 245: 373-383.
4. Bhattacharya R, Fan F, Wang R, Ye X, Xia L, Boulbes D, Ellis LM. Intracrine VEGF signalling mediates colorectal cancer cell migration and invasion. Br J Cancer 2017; 117: 848-855.
5. Blum A, Wang P, Zenklusen JC. SnapShot: TCGA-analyzed tumors. Cell 2018; 173: 530.
6. Brodbelt A, Greenberg D, Winters T, Williams M, Vernon S, Collins VP. Glioblastoma in England: 2007-2011. Eur J Cancer 2015; 51: 533-542.
7. Carthew RW, Sontheimer EJ. Origins and Mechanisms of miRNAs and siRNAs. Cell 2009; 136: 642-655.
8. Chen L, Zeng D, Xu N, Li C, Zhang W, Zhu X, Gao Y, Chen PR, Lin J. Blood-brain barrier- and blood-brain tumor barrier-penetrating peptide-derived targeted therapeutics for glioma and malignant tumor brain metastases. ACS Appl Mater Interfaces 2019; 11: 41889-41897.
9. Chen R, Smith-Cohn M, Cohen AL, Colman H. Glioma subclassifications and their clinical significance. Neurotherapeutics 2017; 14: 284-297.
10. Chiappelli F, Phil AB, Arora R, Phi L, Giroux A, Uyeda M, Kung J, Ramchandani M. Reliability of quality assessments in research synthesis: Securing the highest quality bioinformation for HIT. Bioinformation 2012; 8: 691-694.
11. Du B, Shim JS. Targeting epithelial-mesenchymal transition (EMT) to overcome drug resistance in cancer. Molecules 2016; 21: 965.
12. Grek CL, Sheng Z, Naus CC, Sin WC, Gourdie RG, Ghatnekar GG. Novel approach to temozolomide resistance in malignant glioma: connexin43-directed therapeutics. Curr Opin Pharmacol 2018; 41: 79-88.
13. Hirata T, Kinoshita M, Tamari K, Seo Y, Suzuki O, Wakai N, Achiha T, Umehara T, Arita H, Kagawa N, Kanemura Y, Shimosegawa E, Hashimoto N, Hatazawa J, Kishima H, Teshima T, Ogawa K. 11C-methionine-18F-FDG dual-PET-tracer-based target delineation of malignant glioma: evaluation of its geometrical and clinical features for planning radiation therapy. J Neurosurg 2019; 131: 676-686.
14. Jones PS, Yekula A, Lansbury E, Small JL, Ayinon C, Mordecai S, Hochberg FH, Tigges J, Delcuze B, Charest A, Ghiran I, Balaj L, Carter BS. Characterization of plasma-derived protoporphyrin-IX-positive extracellular vesicles following 5-ALA use in patients with malignant glioma. EBioMedicine 2019; 48: 23-35.
15. Kamarudin MNA, Parhar I. Emerging therapeutic potential of anti-psychotic drugs in the management of human glioma: A comprehensive review. Oncotarget 2019; 10: 3952-3977.
16. Lim S, Kaldis P. CDKs, cyclins and CKIs: roles beyond cell cycle regulation. Development 2013; 140: 3079-3093.
17. Lin AJ, Campian JL, Hui C, Rudra S, Rao YJ, Thotala D, Hallahan D, Huang J. Impact of concurrent versus adjuvant chemotherapy on the severity and duration of lymphopenia in glioma patients treated with radiation therapy. J Neurooncol 2018; 136: 403-411.
18. Lu VM, O'Connor KP, Shah AH, Eichberg DG, Luther EM, Komotar RJ, Ivan ME. The prognostic significance of CDKN2A homozygous deletion in IDH-mutant lower-grade glioma and glioblastoma: a systematic review of the contemporary literature. J Neurooncol 2020; 148: 221-229.

19. Mon-López D, Tejero-González CM. Validity and reliability of the TargetScan ISSF Pistol & Rifle application for measuring shooting performance. Scand J Med Sci Sports 2019; 29: 1707-1712.
20. Pastushenko I, Blanpain C. EMT transition states during tumor progression and metastasis. Trends Cell Biol 2019; 29: 212-226.
21. Pessôa IA, Amorim CK, Ferreira WAS, Sagica F, Brito JR, Othman M, Meyer B, Liehr T, de Oliveira EHC. Detection and correlation of single and concomitant TP53, PTEN, and CDKN2A alterations in gliomas. Int J Mol Sci 2019; 20: 2658.
22. Qi X, Wan Y, Zhan Q, Yang S, Wang Y, Cai X. Effect of CDKN2A/B rs4977756 polymorphism on glioma risk: a meta-analysis of 16 studies including 24077 participants. Mamm Genome 2016; 27: 1-7.
23. Schafer KA. The cell cycle: a review. Vet Pathol 1998; 35: 461-478.
24. Schill R, Solbrig S, Wettig T, Spang R. Modelling cancer progression using Mutual Hazard Networks. Bioinformatics 2020; 36: 241-249.
25. Serra S, Chetty R. p16. J Clin Pathol 2018; 71: 853-858.
26. Sibin MK, Bhat DI, Narasingarao KV, Lavanya C, Chetan GK. CDKN2A (p16) mRNA decreased expression is a marker of poor prognosis in malignant high-grade glioma. Tumour Biol 2015; 36: 7607-7614.
27. Srivastava C, Irshad K, Dikshit B, Chattopadhyay P, Sarkar C, Gupta DK, Sinha S, Chosdol K. FAT1 modulates EMT and stemness genes expression in hypoxic glioblastoma. Int J Cancer 2018; 142: 805-812.
28. Sun X, Ma X, Wang J, Zhao Y, Wang Y, Bihl JC, Chen Y, Jiang C. Glioma stem cells-derived exosomes promote the angiogenic ability of endothelial cells through miR-21/VEGF signal. Oncotarget 2017; 8: 36137-36148.
29. Wang L, He S, Yuan J, Mao X, Cao Y, Zong J, Tu Y, Zhang Y. Oncogenic role of SOX9 expression in human malignant glioma. Med Oncol 2012; 29: 3484-3490.
30. Xiong L, Wang F, Qi Xie X. Advanced treatment in high-grade gliomas. J BUON 2019; 24: 424-430.
31. Yang BY, Song JW, Sun HZ, Xing JC, Yang ZH, Wei CY, Xu TY, Yu ZN, Zhang YN, Wang YF, Chang H, Xu ZP, Hou M, Ji MJ, Zhang YS. PSMB8 regulates glioma cell migration, proliferation, and apoptosis through modulating ERK1/2 and PI3K/AKT signaling pathways. Biomed Pharmacother 2018; 100: 205-212.
32. Yang L, Lin C, Jin C, Yang JC, Tanasa B, Li W, Merkurjev D, Ohgi KA, Meng D, Zhang J, Evans CP, Rosenfeld MG. lncRNA-dependent mechanisms of androgen-receptor-regulated gene activation programs. Nature 2013; 500: 598-602.
33. Yang Y, Duan W, Liang Z, Yi W, Yan J, Wang N, Li Y, Chen W, Yu S, Jin Z, Yi D. Curcumin attenuates endothelial cell oxidative stress injury through Notch signaling inhibition. Cell Signal 2013; 25: 615-629.
34. Yi R, Feng J, Yang S, Huang X, Liao Y, Hu Z, Luo M. miR-484/MAP2/c-Myc-positive regulatory loop in glioma promotes tumor-initiating properties through ERK1/2 signaling. J Mol Histol 2018; 49: 209-218.
35. Yu L, Xu J, Liu J, Zhang H, Sun C, Wang Q, Shi C, Zhou X, Hua D, Luo W, Bian X, Yu S. The novel chromatin architectural regulator SND1 promotes glioma proliferation and invasion and predicts the prognosis of patients. Neuro Oncol 2019; 21: 742-754.
36. Zhang M, Liu S, Guan E, Liu H, Dong X, Hao Y, Zhang X, Zhao P, Liu X, Pan S, Wang Y, Wang X, Liu Y. Hyperbaric oxygen therapy can ameliorate the EMT phenomenon in keloid tissue. Medicine (Baltimore) 2018; 97: e11529.
37. Zhang Q, Cao YF, Ran RX, Li RS, Wu X, Dong PP, Zhang YY, Hu CM, Wang WM. Strong specific inhibition of UDP-glucuronosyltransferase 2B7 by atractylenolide I and III. Phytother Res 2016; 30: 25-30.